Author Manuscript

Author Manuscript

Author Manuscript

Author Manuscript

HHS Public Access

Author manuscript

Oncogene. Author manuscript; available in PMC 2018 May 04.

Published in final edited form as:

Oncogene. 2012 January 12; 31(2): 200–212. doi:10.1038/onc.2011.231.

TRPV4 mediates tumor-derived endothelial cell migration via arachidonic acid-activated actin remodeling

A Fiorio Pla[1,2,3], **HL Ong**[4], **KT Cheng**[4], **A Brossa**[1,5], **B Bussolati**[5], **T Lockwich**[4], **B Paria**[4], **L Munaron**[1,2,3], and **IS Ambudkar**[4]

[1]Department of Animal and Human Biology, University of Torino, Torino, Italy

[2]Center for Complex Systems in Molecular Biology and Medicine (SysBioM), Torino, Italy

[3]Nanostructured Interfaces and Surfaces Centre of Excellence, Torino, Italy

[4]Secretory Physiology Section, Molecular Physiology and Therapeutics Branch, NIDCR, NIH, Bethesda, MD, USA

[5]Department of Internal Medicine, Centre for Molecular Biotechnology, University of Torino, Torino, Italy

Abstract

Changes in intracellular calcium $[Ca^{2+}]_i$ levels control critical cytosolic and nuclear events that are involved in the initiation and progression of tumor angiogenesis in endothelial cells (ECs). Therefore, the mechanism(s) involved in agonist-induced Ca_i^{2+} signaling is a potentially important molecular target for controlling angiogenesis and tumor growth. Several studies have shown that blood vessels in tumors differ from normal vessels in their morphology, blood flow and permeability. We had previously reported a key role for arachidonic acid (AA)-mediated Ca^{2+} entry in the initial stages of tumor angiogenesis *in vitro*. In this study we assessed the mechanism involved in AA-induced EC migration. We report that TRPV4, an AA-activated channel, is differentially expressed in EC derived from human breast carcinomas (BTEC) as compared with 'normal' EC (HMVEC). BTEC display a significant increase in TRPV4 expression, which was correlated with greater Ca^{2+} entry, induced by AA or 4αPDD (a selective TRPV4 agonist) in the tumor-derived ECs. Wound-healing assays revealed a key role of TRPV4 in regulating cell migration of BTEC but not HMVEC. Knockdown of TRPV4 expression completely abolished AA-induced BTEC migration, suggesting that TRPV4 mediates the pro-angiogenic effects promoted by AA. Furthermore, pre-incubation of BTEC with AA induced actin remodeling and a subsequent increase in the surface expression of TRPV4. This was consistent with the increased plasma membrane localization of TRPV4 and higher AA-stimulated Ca^{2+} entry in the migrating cells. Together, the data presented herein demonstrate that: (1) TRPV4 is differentially expressed in tumor-derived versus 'normal' EC; (2) TRPV4 has a critical role in the migration of tumor-

Correspondence: Dr A Fiorio Pla, Department of Animal and Human Biology, University of Torino, V. Accademia Albertina 13, 10123 Torino, Italy. alessandra.fiorio@unito.it.

Conflict of interest

The authors declare no conflict of interest.

Supplementary Information accompanies the paper on the Oncogene website (http://www.nature.com/onc)

Author Manuscript Author Manuscript Author Manuscript Author Manuscript

derived but not 'normal' EC migration; and (3) AA induces actin remodeling in BTEC, resulting in a corresponding increase of TRPV4 expression in the plasma membrane. We suggest that the latter is critical for migration of EC and thus in promoting angiogenesis and tumor growth.

Keywords

Ca^{2+} signals; TRP channels; endothelial cells; cell migration; actin remodeling; tumor angiogenesis

Introduction

Angiogenesis, defined as the formation of new capillaries from pre-existing ones, has a key role in growth and development of blood vessels, as well as in wound healing. Nonetheless, angiogenesis is also fundamental in pathological processes, such as cancer, in which the development of new blood vessels is critical for tumor growth as well metastasis. Tumor angiogenesis is mediated by the secretion of a large number of growth factors by tumor cells. These growth factors in turn stimulate endothelial cells (ECs) within the tumor to sprout, proliferate, migrate and finally differentiate into new blood vessels (Folkman, 2003; Carmeliet, 2005). Endothelial cells were previously considered to be genetically stable when compared with tumor cells and therefore, were an ideal therapeutic target in the development of anti-angiogenic treatments. However, their stability has been questioned with several studies showing that tumor-derived EC (TEC) differ significantly from their normal counterparts at genetic and functional levels (St Croix *et al.*, 2000; Hida *et al.*, 2004; Bussolati *et al.*, 2011). Gene expression profiles obtained using microarrays and quantitative PCR revealed that tumor vasculature express unique markers that distinguish them from normal EC (St Croix *et al.*, 2000; Bussolati *et al.*, 2003; Bhati *et al.*, 2008). Furthermore, TEC from human melanoma, liposarcoma and breast carcinoma are resistant to apoptosis; in particular those from breast (BTEC) and renal (RTEC) carcinomas exhibit enhanced angiogenic properties and display an immature/embryonic phenotype (Bussolati *et al.*, 2003; Grange *et al.*, 2006). The molecular mechanisms that are involved in promoting tumor growth and metastasis are still not well understood. Thus, studies focused directly on understanding the regulation of TEC function may provide useful information for development of TEC-based therapies.

Intracellular calcium ($Ca^{2+}{}_i$) signaling is a highly conserved and ubiquitous mechanism that controls various processes including cell survival, proliferation, motility, apoptosis and differentiation. Importantly, $Ca^{2+}{}_i$ signaling is critically involved in the regulation of angiogenesis (Patton *et al.*, 2003; Munaron and Fiorio Pla, 2009; Prevarskaya *et al.*, 2010). We recently showed that arachidonic acid (AA), a lipid second messenger released by different pro-angiogenic factors (such as basic fibroblast growth factor and vascular endothelial growth factor), is actively involved in the early steps of the angiogenic process *in vitro* and mediates its effects by activating Ca^{2+} entry via Ca^{2+}-permeable plasma membrane channels. Carboxy-amidotriazole, an inhibitor of Ca^{2+} entry and angiogenesis, has been shown to significantly and specifically decrease AA-induced tubulogenesis and Ca^{2+} entry in BTEC (Fiorio Pla *et al.*, 2008). However, the molecular nature of the plasma membrane

Author Manuscript Author Manuscript Author Manuscript Author Manuscript

channel(s) mediating such Ca^{2+} entry in BTEC is still unknown. The discovery of transient receptor potential (TRP) superfamily of channels provided putative candidates for non-voltage-gated Ca^{2+} entry mechanisms, including Ca^{2+} entry channels induced by store depletion, mechanical stretch or second messengers such as inositol 1,4,5-trisphosphate or AA (Nilius *et al.*, 2007; Birnbaumer, 2009). Several TRP channels have been identified in a variety of ECs, for example, TRPC1, TRPC4, TRPC6, TRPV1 and TRPV4 (Kwan *et al.*, 2007; Everaerts *et al.*, 2010). These channels appear to be differentially expressed in different types of ECs and show varying contributions to agonist-induced or mechanical stretch-induced Ca^{2+} entry (Meves, 2008; Everaerts *et al.*, 2010). In particular, TRPV4 (also called OTRPC4, TRP12 and VR-OAC) was shown to be distributed in a broad range of tissues including vascular endothelium, trachea, kidney, liver, heart, lung, testis, brain and ears. Although TRPV4 was initially described as being mainly activated by hypotonicity, it is now well known that it can be activated by mechanical stresses (for example, membrane stretch), chemical stimuli such as phorbol ester derivates (for example, 4α-Phorbol 12, 13-didecanoate (4αPDD), a specific agonist for TRPV4) or endogenous stimuli such as AA and its metabolites (Gao *et al.*, 2003; Liedtke and Kim, 2005; Mutai *et al.*, 2005) and has been shown to be expressed and functional in vascular endothelium. TRPV4 has been implicated in the regulation of vascular tone in large arteries (Hartmannsgruber *et al.*, 2007) and is critical in mediating the shear-stress responses of microvessels and subsequent reorientation of ECs (Thodeti *et al.*, 2009). We have previously shown that AA-mediated Ca^{2+} entry is critical in the early events associated with TEC angiogenesis. AA directly or indirectly (via metabolites) activates several different calcium channels, including TRP channels from the TRPV and TRPM subfamilies. Of these TRPV4 has been proposed to be directly activated by epoxyeicosatrienoic acids, which are AA metabolites (Watanabe *et al.*, 2003; Meves, 2008; Everaerts *et al.*, 2010). In the present study we have elucidated the Ca^{2+} channel targeted by AA that is involved in migration of TEC.

Herein, we report that the expression of endogenous TRPV4 is significantly higher in BTEC compared with ‘normal’ ECs (HMVEC). TRPV4 has a key role in mediating Ca^{2+} entry in BTEC as loss of TRPV4 expression resulted in decreased $Ca^{2+}{}_i$ responses to 4αPDD and complete inhibitions of AA-induced migration of BTEC. Finally, AA induced actin remodeling and increased surface expression of TRPV4 in BTEC. The latter was strongly displayed by migrating cells. Thus, our findings reveal that AA regulates angiogenesis by inducing remodeling of the cytoskeleton and stimulating TRPV4 channel activity, both of which are critical for TEC migration.

Results

Tumor-derived endothelial cells display high expression and function of TRPV4

BTECs were used in the present study as these cells represent a very good model to study tumor vascularization properties compared with normal tissue vascularization (Grange *et al.*, 2006). Previous studies reported that migration of BTEC is greater than that of normal ECs (Grange *et al.*, 2006). This is further demonstrated in Figure 1a using the wound-healing assay. BTEC displayed a higher migration rate as compared with normal human microvascular ECs isolated from derma (HMVEC-d) both in serum-free conditions and in

Author Manuscript Author Manuscript Author Manuscript Author Manuscript

endothelial basal medium (EBM) medium (both cell types displayed higher migration in the latter). Note that although HMVEC showed minimal migration in serum-free medium, BTEC displayed higher spontaneous migration. It should be noted that the total absence of serum was not optimal for the culture of HMVEC-d and therefore, subsequent experiments were conducted using in 2% fetal bovine serum as basal condition. As Ca^{2+} entry plays a critical role in EC migration, we examined whether BTEC and HMVEC were different in this aspect. Based on the reported role for AA in angiogenesis, we examined AA-induced Ca^{2+} mobilization in both cell types. Although AA induced an increase in intracellular Ca^{2+} concentration ($[Ca^{2+}]_i$) in both cell types, the increase in BTEC was significantly more than in the normal cells (Figures 1bi and biii). We have previously demonstrated that this $[Ca^{2+}]_i$ increase is completely abolished in Ca^{2+}-free medium, suggesting that a major portion of it was due to extracellular Ca^{2+} entry (Fiorio Pla and Munaron, 2001; Fiorio Pla *et al.*, 2008). To determine whether TRPV4 mediates this Ca^{2+} entry, the TRPV4-specific agonist 4αPDD was used. As seen with AA, BTEC also demonstrated higher $[Ca^{2+}]_i$ elevation than normal cells following 4αPDD stimulation (Figures 1bii and biii). Thus, both AA- and 4αPDD-induced Ca^{2+} responses were higher in BTEC compared with HMVEC.

Endogenous TRPV4 expression has been reported in different types of ECs (both primary cells as well as cell lines) (Everaerts *et al.*, 2010). As shown in Figure 1c, the expression of endogenous TRPV4 was markedly higher in BTEC compared with HMVEC-d or ECs isolated from cardiac microvasculature (HMVEC-c). To assess whether increased endogenous TRPV4 expression was a common feature of TEC, protein expression in RTEC was compared with normal kidney glomerular EC (GEC). Expression of endogenous TRPV4 was also higher in RTEC compared with ‘normal’ GEC (Figure 1c).

Knocking down TRPV4 significantly reduced the peak amplitude of 4αPDD-induced Ca^{2+} responses in BTEC (cf control, untransfected BTEC; Figures 1di and diii). On the other hand, overexpression of TRPV4 in HMVEC-d significantly enhanced 4αPDD-induced Ca^{2+} responses (Figures 1dii and diii). Interestingly, the peak amplitude of TRPV4-mediated Ca^{2+} responses in HMVEC-d overexpressing TRPV4 was very similar (not statistically different) to that measured in BTEC. The extent of TRPV4 knockdown by shTRPV4 is shown in Supplementary Figure S1D (transfection with shTRPV4 for 72 h induced > 50% knockdown of TRPV4 expression). In aggregate, the data in Figure 1 demonstrate that the expression and function of endogenous TRPV4 are significantly increased in TEC when compared with normal ECs.

TRPV4 activation is involved in AA-mediated tumor-derived endothelial cell migration

We then evaluated the role of TRPV4 in mediating EC migration using its specific agonist, 4αPDD. At each time point measured, BTEC consistently had a higher basal (that is, in 2% fetal bovine serum alone, CNTRL−) as well as serum-stimulated (EBM, CNTRL+) rate of cell migration than HMVEC-d (Figure 2). Further, when stimulated with 10 μM 4αPDD, BTEC migrated at a significantly faster rate than unstimulated cells. Notably, 4αPDD did not have any stimulatory effect on the migration rate of HMVEC-d (Figures 2a and b). We have previously shown that AA-induced Ca^{2+} entry promotes the organization of BTEC into vessel-like structures *in vitro*, a phenomenon that is partly dependent on cell migration

Author Manuscript Author Manuscript Author Manuscript Author Manuscript

(Fiorio Pla *et al.*, 2008). HMVEC migration, on the other hand, was not effected by AA (Fiorio Pla *et al.*, 2010). Thus, wound-healing assays were conducted with BTEC to further confirm the role of AA on EC migration. After incubating the cells with AA (5 μM) for at least 4 h, a significant increase in the migration rates of EC was observed (Figure 3). Inhibiting TRPV4 channel activity using ruthenium red (1 μM), a pan-TRPV channel antagonist shown to block TRPV4 (Watanabe *et al.*, 2002; Gao *et al.*, 2003), completely abolished AA-induced B-TEC migration (Figures 3a and bi). Similarly, knocking down TRPV4 expression also completely abolished the pro-migratory effect of 5 μM AA and 10 μM 4αPDD on BTEC transfected with shTRPV4 (c.f. cells transfected with an empty short hairpin RNA (shRNA) vector) (Figures 3a and bii). These data suggest that TRPV4-mediated Ca^{2+} entry is required for AA-induced BTEC migration.

To further demonstrate TRPV4 involvement in EC migration, we analyzed TRPV4-mediated Ca^{2+} signaling in migrating versus non-migrating cells. 4αPDD-induced Ca^{2+} responses were compared in confluent (non-migrating) and migrating BTEC (the latter line the wound in a wound-healing assay) (Figure 4). Importantly, the migrating cells showed significantly higher 4αPDD-induced Ca^{2+} responses on average when compared with confluent, non-migrating cells ($n = 13$ experiments; $P < 0.05$). Together these data demonstrate that TRPV4 has an important role in the migration of BTEC and potentially in tumor progression and metastasis.

AA synchronizes TRPV4-mediated Ca^{2+} responses

To determine possible effects of AA on TRPV4, BTEC were stimulated with 10 μM 4αPDD either before or after treatment with AA. 4αPDD induced asynchronous Ca^{2+} i responses in BTEC, which displayed a wide latency distribution (time taken for cells to respond to 4αPDD stimulation) ranging between 0 and 390 s with a median value of 240 s and a mean value of 207 s (Figures 5ai, b and c). As a point of comparison, uridine triphosphate (UTP, 10 μM) was added after near complete cessation of 4αPDD-induced responses. However, unlike 4αPDD, UTP induced rapid and simultaneous Ca^{2+} i increase in all the cells. Interestingly, pre-incubation with 5 μM AA resulted in synchronization of the 4αPDD-induced Ca^{2+} responses, without affecting the UTP responses. AA-treated cells displayed a greatly reduced latency distribution (max = 108 s, median = 18 s, mean = 58 s; Figures 5aii, b and c).

As TRPV4 function has been shown to depend on an intact cytoskeleton (Liu *et al.*, 2006; Becker *et al.*, 2009), we hypothesized that the AA-induced synchronization of Ca^{2+} responses in BTEC maybe be caused by changes in the actin cytoskeleton. Thus, we examined the effect of actin depolymerization on TRPV4-mediated Ca^{2+} responses in AA-treated BTEC. Treatment with 1 μM cytochalasin D (pre-incubation for 30 min at 37 °C) prevented the AA-induced synchronization of 4αPDD-induced Ca^{2+} responses in BTEC (Figure 5aiii) with a corresponding increase in the range of latency distribution from 0 to 342 s with a mean value of 109.5 s and a median value of 90 s (very similar to the range obtained with 4αPDD stimulation alone; Figures 5b and c). These novel data suggest that AA synchronizes TRPV4—mediated Ca^{2+} responses in BTEC likely by inducing actin remodeling.

Author Manuscript Author Manuscript Author Manuscript Author Manuscript

Remodeling of the actin cytoskeleton increased endogenous TRPV4 expression at the plasma membrane

To provide further evidence for the role of actin remodeling in AA-induced synchronization of TRPV4-mediated Ca^{2+} responses in BTEC, F-actin stress fibers were detected using phalloidin in BTEC expressing TRPV4-GFP. In untreated control cells, the network of actin stress fibers could be clearly detected in cells immobilized on a substrate (that is, gelatin) through focal adhesion formation (Figure 6Ai, left panels). Pre-incubation with 5 μM AA (10 min at 37 °C) induced remodeling of the actin cytoskeleton, resulting in partial disappearance of stress fibers and a concentration of actin in the cell periphery (Figure 6Ai, right panels). This is in agreement with the pro-migratory role of AA as actin remodeling and partial rearrangement of stress fibers in cortical actin are required for cell migration. Using a plot profile traced along the major cell axis, the fluorescence signal for phalloidin was diffusely distributed in untreated control cells (Figure 6Aii, left graph). However, in cells pre-incubated with AA, the actin/ phalloidin signal was mostly localized in the cell periphery (Figure 6Aii, right graph). Furthermore, AA-stimulated BTEC appeared to have a significantly smaller cell surface area (729 μm^2, $n = 121$ cells; $P < 0.001$) compared with control, unstimulated cells (1011 μm^2, $n = 103$ cells). Again, this data are consistent with the cytoskeletal rearrangement and consequent pro-migratory effect of AA on the cells. Activation of TRPV4 by 4αPDD does not affect actin (Supplementary Figure S3). Moreover, TRPV4 is not recruited to the plasma membrane of BTEC when the actin cytoskeleton is disrupted by cytochalasin D treatment *per se* (data not shown).

Pre-incubating BTEC with AA markedly increased the amount of TRPV4-GFP in the plasma membrane (Figure 6Bi, compare left and right panels). Figures 6Bii and Biii show the quantification of TRPV4-GFP in the plasma membrane region. The fluorescence intensity of TRPV4-GFP was traced along the axis of the cells using a plot profile. The green fluorescence protein (GFP) fluorescence signal was diffusely distributed throughout the cytoplasm in untreated control cells (Figures 6Bi and Bii; left panel and graph). Following AA treatment, TRPV4-GFP was predominantly localized in the cell periphery as indicated by a higher fluorescence signal at both ends of the plot profile (Figure 6Bii; left panel and graph). There was a clear and significant decrease of TRPV4-GFP fluorescence signal inside the cell, indicating that TRPV4-GFP was trafficked from the cytoplasm to the plasma membrane following AA stimulation (Figure 6Biii). More importantly, there was clear colocalization of TRPV4-GFP with the actin/phalloidin fluorescent signal in BTEC (Figure 6C, panels c–d and g–h). In resting, unstimulated cells, actin and TRPV4-GFP were diffusely localized in the cytoplasm with minimal localization in the plasma membrane of some cells (Figure 6C, panels a and b). Following AA treatment, TRPV4-GFP was trafficked on the plasma membrane region where it strongly colocalized with the cortical actin (Figure 6C, panels e and f). Furthermore, surface biotinylation assays were performed in control and AA-treated BTEC. There was a significant increase in the surface expression of TRPV4 following AA treatment, compared with untreated control cells (Figure 7). Together these findings demonstrate that, in addition to possible direct effects on TRPV4 channel activity, AA also increases the expression of TRPV4 channels in the plasma membrane by inducing remodeling of the actin cytoskeleton. The net result is an overall increase in active TRPV4 channels.

Author Manuscript Author Manuscript Author Manuscript Author Manuscript

Discussion

Among the second messengers released upon stimulation of ECs with pro-angiogenic factors (such as basic fibroblast growth factor or vascular endothelial growth factor), the fatty acid AA and its metabolites promote the generation of $Ca^{2+}{}_i$ signals that are required for cell proliferation and migration and neo-angiogenesis (Fiorio Pla and Munaron, 2001; Nie and Honn, 2002; Antoniotti *et al.*, 2003; Hyde and Missailidis, 2009). We had previously shown that AA plays a key role in the formation of 'capillary-like structure' by tumor-derived endothelial cells, BTEC (Fiorio Pla *et al.*, 2008). In the present paper, we studied the molecular mechanism involved in AA-mediated pro-angiogenic effect and report for the first time that the non-selective cation channel, TRPV4, has an important role in mediating AA-induced cell migration and Ca^{2+} entry in TEC.

Although several studies have demonstrated the importance of agonist-stimulated $Ca^{2+}{}_i$ signaling in the angiogenic process, very little is known about the molecular nature of the channels involved in mediating these responses. Recent evidence suggests a role for TRPC channels in vascular endothelial growth factor-induced Ca^{2+} responses and vascular permeability (Pocock *et al.*, 2004). TRPC6 has been shown to be a critical component of the channels mediating cation entry in response to vascular endothelial growth factor and 1-oleoyl-2-acetyl-sn-glycerol (OAG) in HMVEC (Hamdollah Zadeh *et al.*, 2008). Yu *et al.* (2010) reported that knockdown of TRPC1 caused severe angiogenic defects in intersegmental vessel sprouting of zebrafish, indicating that TRPC1 is required for angiogenesis *in vivo*. We proposed that the TRPV4 channel is a good candidate to mediate BTEC migration as the channel is activated in responses to changes in cell morphology, such as during cell swelling and shear stress. TRPV4 is also activated by endogenous compounds such as AA and its metabolites (for example, epoxyeicosatrienoic acids), which are important inflammatory messengers that may mediate migration of ECs toward sites of inflammation (Everaerts *et al.*, 2010). Furthermore, TRPV4 is widely expressed in the vascular endothelium in which it has been shown to function as a sensor for shear stress. The channel acts as a mechanosensor activated by mechanical stretching of ECs sensing the fluid shear stress that also regulates cell re-orientation, whereas in larger arteries it functions as a key factor in shear stress-induced vasodilation (Hartmannsgruber *et al.*, 2007; Thodeti *et al.*, 2009). Both shear stress and agonist-activation of TRPV4 stimulate proliferation of ECs and trigger collateral growth after arterial occlusion (Troidl *et al.*, 2009). On the other hand, the possible role of TRPV4 in cell migration has only been recently reported. Although TRPV1 had a predominant role in regulating migration of hepatoblastoma HepG2 cells, activation of TRPV4 channels resulted in increased lamellopodial dynamics that was reflected as a rise in the cell velocity (Waning *et al.*, 2007). In addition, Thodeti *et al.* (2009) had previously demonstrated that TRPV4 is a mechanosensor activated by mechanical stretching of ECs and regulates cell reorientation, a key element in the directional migration and oriented sprouting that drive angiogenesis.

Data from the present study show that TRPV4 has a central role in the regulation of BTEC migration. We report that both expression of TRPV4 and 4α.PDD-mediated Ca^{2+} entry is increased in BTEC when compared with normal microvascular ECs. In this regard, it is interesting to note that increased endogenous TRPV4 expression is not restricted to BTECs

Author Manuscript Author Manuscript Author Manuscript Author Manuscript

and is also found in ECs derived from renal carcinomas. The pro-migratory effect of TRPV4 stimulation, by either 4αPDD or AA, on BTEC represents a direct link between TRPV4 and AA-mediated cell migration. Moreover, we demonstrate a clear 'positional effect' of TRPV4-mediated $[Ca^{2+}]_i$ signaling in migrating versus non-migrating cells. The data are in accordance with our previous report that AA-mediated Ca^{2+} responses are involved in early stages of capillary-like structure organization of BTEC (Fiorio Pla *et al.*, 2008). Although the molecular mechanism responsible for organizing the capillary structure is not yet known, we propose that migrating cells at the leading edges have higher Ca^{2+} 'responsiveness' and that could be, at least in part, due to AA-induced actin remodeling and a consequent increase in the trafficking of TRPV4 to the plasma membrane. As a result, there are more TRPV4 channels in the surface membrane of these cells and Ca^{2+} entry via these channels drives the migration of BTEC.

Previous studies have shown that AA metabolites affect actin dynamics by inducing an increase in actin polymerization (Peppelenbosch *et al.*, 1995a, b; Moes *et al.*, 2010). AA and its metabolites activate signaling pathways that lead to the activation of GTPases such as Rac and Rho, ultimately resulting in actin remodeling (Peppelenbosch *et al.*, 1995a; Shin *et al.*, 1999). In some studies, AA and some of its metabolites have been shown to bind directly to and regulate the activity of specific GTPase-activating proteins, which are in turn regulators of small GTPases (Tsai *et al.*, 1989; Roberts *et al.*, 2003). Involvement of the cytoskeleton in regulation of TRPV4 channels has been previously reported. TRPV4 colocalized with actin in the keratinocyte-derived permanent cell line and this interaction was important for activation of TRPV4 by hypotonic cell swelling (Becker *et al.*, 2005). Similar results were obtained with human submandibular gland cells in which inhibition of actin remodeling impaired the hypotonic stress-induced trafficking of TRPV4 to the plasma membrane (Liu *et al.*, 2006). It was also shown that MAP-7 may mediate the interaction between TRPV4 and the actin cytoskeleton as TRPV4 interacts with MAP-7 via its C terminus and this interaction facilitates the expression of TRPV4 on the cell surface (Suzuki *et al.*, 2003). In addition, another recent study reported a direct interaction of TRPV4 with the actin cytoskeleton (Goswami *et al.*, 2010). It is also interesting to note that TRPV4, like TRPV1 and TRPV2, translocates to the plasma membrane in response to the agonist stimulation in cultured cells. Thus, regulated trafficking appears to be a common mechanism underlying the activation of TRPV channels by specific cellular stimulus/signals (Boels *et al.*, 2001; Morenilla-Palao *et al.*, 2004; Van Buren *et al.*, 2005; Liu *et al.*, 2006). In this regard, Ma *et al.* (2010) recently showed that TRPV4-TRPC1 heteromeric channel trafficking to the plasma membrane is enhanced by Ca^{2+} store depletion in human umbilical vein ECs. It would be interesting to elucidate the contribution of TRPC1 in BTEC as in addition to TRPV4, these cells also express TRPC1 (data not shown). It is also important to note that our data do not exclude a role for AA metabolites, as has been reported for epoxyeicosatrienoic acid (Watanabe *et al.*, 2003), in direct activation of TRPV4 in addition to increasing AA-mediated channel activity due to remodeling of the actin cytoskeleton and plasma membrane recruitment of the channel. Presently we have not clarified the exact AA metabolites involved in TRPV4 activation and actin remodeling. Nevertheless, the data demonstrate that TRPV4 surface expression is dependent on AA-induced actin remodeling,

Author Manuscript Author Manuscript Author Manuscript Author Manuscript

not *vice versa*. Once inserted the channel could be activated by epoxyeicosatrienoic acid or other AA metabolites.

In conclusion, the findings presented above demonstrate a role for TRPV4 in mediating the migration of TEC, which is one of the key processes involved in the neovascularization of tumors. Furthermore, AA-induced TRPV4 activation and cell migration is dependent on AA-induced remodeling of the actin cytoskeleton. Our data show that this cytoskeletal change facilitates TRPV4 trafficking to the plasma membrane in which it is activated.

Together our study reveals that TRPV4 channel is a potentially critical therapeutic target for the development of novel anti-angiogenic treatment strategies for breast tumors.

Materials and methods

Cell culture, transfection and plasmid construction

Tumor-derived ECs were obtained from breast lobular-infiltrating carcinoma (BTEC) or from specimens of RTEC. Endothelial cells were isolated, using anti-CD105 antibody coupled to magnetic beads, by magnetic cell sorting using the MACS system (Miltenyi Biotec, Auburn, CA, USA) and grown in complete EBM medium (Lonza, East Rutherford, NJ, USA) supplemented with 10% fetal calf serum (FCS) (Lonza), 50 μg/ml gentamycin (Lonza) and 2mM glutamine (Lonza) as previously described (Bussolati *et al.*, 2006; Grange *et al.*, 2006). Cells were used at passages 3–15. Primary microvascular EC lines obtained from GEC were prepared as previously described (Collino *et al.*, 2008). Briefly, human glomeruli were purified from specimens of normal renal tissue obtained for polar carcinomas by passages on sequential meshes, digested by trypsin (0.1%, 30 min at 37 °C), and plated onto gelatin in complete EBM medium. After 1 week, cells were detached and ECs were purified by using an anti-CD31 antibody coupled to magnetic beads by magnetic cell sorting using the MACS system (Miltenyi Biotec). To confirm their identity, BTEC, RTEC and GEC were characterized by cell morphology, expression of a panel of endothelial antigens (for example, CD105, CD31, Muc-18 (CD146), CD44 and VEGFR2 (KDR)), positive staining for the von Willebrand factor antigen and negative staining for cytokeratin and desmin (Grange *et al.*, 2006). Adult human dermal microvascular ECs (HMVEC-d) and adult human cardiac microvascular ECs (HMVEC-c) were purchased from Lonza and grown in EGM2-MV medium (Lonza). Cells were used at passages 3–10.

BTEC and HMVEC cells were transfected using the Amaxa Basic Nucleofector Kit for mammalian ECs according to the instructions of the manufacturer using the M-003 program for B-TEC or S-005 for HMVEC-d (Lonza). Overall, 1×10^6 B-TEC or 0.5×10^6 HMVEC-d cells were transfected with 3 μg shTRPV4 or 1.5 μg TRPV4-GFP (as indicated in the text and figures). The shTRPV4 construct was made using the following sense (5′-CACCGATCTGCTGGAGTCCACCCTA CGAATAGGGTGGACTCCAGCAGATC-3′) and antisense (5′-AAAAGATCTGCTGGAGTCCACCCTATTCGTAGGG TGGACTCCAGCAGATC-3′) oligonucleotides. The corresponding control shRNA with a scrambled sequence was made using the sense (5′-GATCTTGGTCGTGCGCTCTTA-3′) and antisense (5′-TAAGAGCGCACGACCAAGATC-3′) oligonucleotides. To enable directional cloning, both sense and antisense oligonucleotides had four nucleotides

Author Manuscript Author Manuscript Author Manuscript Author Manuscript

overhangs at the 5′ end. These two oligonucleotides were hybridized in equal molar ratio and cloned into pENTR/U6 vector. Sequence identity of the cloned plasmids was then confirmed by sequencing. The shTRPV4 was used in TRPV4 silencing experiments, whereas the scrambled shRNA or empty shRNA vectors were used as negative controls. Cells were transfected with 3 μg of these shRNAs for 72 h. For TRPV4-GFP construct, the TRPV4 DNA sequence was cloned in pAcGFP1-N1 vector. The shTRPV4 and TRPV4-GFP constructs were first assessed in western blot and Ca^{2+} imaging experiments before being used in subsequent experiments (Supplementary Figure S1). Lysates of HEK293 cells expressing TRPV4-GFP showed the expected ~100KDa band and a lower ~70kDa band, which may correspond to endogenous TRPV4 (Supplementary Figure S1C). For the experiments showed in Supplementary Figure S3, BTEC were transfected with 1.5 μg of β-actin-mCherry vector (a kind gift from Dr Yamada) as described above.

Protein extraction and western blot analysis

BTEC, RTEC and GEC were grown in EBM containing 10% FCS, whereas HMVEC were grown in EBM-2-MV medium until cells were 80% confluent. Cells were then detached, suspended in ice-cold 1× phosphate-buffered saline containing the following protease inhibitors: 2 μg/ml aprotinin, 1mM Na orthovanadate, 0.1mM PMSF and 10mM NaF. Cells were centrifuged for 15 min at 1000 *g*, and resuspended in a lysis buffer containing (in mM): 100 Tris–HCl (pH 8.0), 1 $MgCl_2$, in the presence of protease inhibitors and frozen at −80 °C for at least 2 h before use. Cells were subjected to one freeze–thaw cycle in the lysis buffer mixed with 2× sucrose solution to give a final concentration of 250mM sucrose, and then homogenized by passing through a syringe tip. Protein concentration was determined using the Quanti-iT protein assay (Invitrogen, Carlsbad, CA, USA) following manufacturer instructions.

Conditions for SDS–PAGE and western blotting were as described previously (Fiorio Pla *et al.*, 2005). Polyvinylidene fluoride membranes were blocked and incubated for 2 h with rabbit anti-TRPV4 antibody (1:200) and the mouse IgG2a anti-β-actin (Sigma, St Louis, MO, USA) antibodies. The membrane was then washed with 1 × TBS containing 0.1% Tween 20 and incubated as required with the HRP-conjugated anti-mouse or anti-rabbit IgG antibodies (Amersham, Piscataway, NJ, USA). Electrochemiluminescence was conducted using the SuperSignal West Pico chemiluminescent substrate (Pierce, Rockford, IL, USA). The anti-TRPV4 antibody was raised against the peptide C-DGHQQGYAPKWRAEDAPL in rabbits (Loftstrand Labs, Gaithersburg, MD, USA). The resulting rabbit serum was then affinity purified to obtain the anti-TRPV4 antibody. Specificity of the anti-TRPV4 antibody was determined using the TRPV4 peptide and comparing its detection of TRPV4 with the two commercial TRPV4 antibodies (Chemicon (Billerica, MA, USA) and Alomone (Jerusalem, Israel) TRPV4 antibodies; Supplementary Figure S2). To quantify the differences in protein expression, the ratio between TRPV4 and actin expression was evaluated. One-way analysis of variance was performed to analyze data sets. *Post-hoc* tests were used to determine statistically significant differences among the groups (Student–Newman–Keuls test).

Author Manuscript Author Manuscript Author Manuscript Author Manuscript

Wound-healing assays

Cell motility was investigated in terms of cell migration into a wound introduced in a confluent monolayer. Cells were grown to confluence on 24-well culture plates coated with 1% gelatin. BTEC were serum-starved for 24 h in Dulbecco's modied Eagle's medium containing 2% FCS. A 'wound' was made under standard conditions by scraping the middle of the cell monolayer with a P10 pipette tip. Floating cells were removed by washing with 1 × phosphate-buffered saline, and the fresh Dulbecco's modied Eagle's medium (DMEM, serum-free for experiments conducted on BTEC or containing 2% FCS for the experiments conducted on HMVEC-d), with or without stimuli, was added (as indicated in the text or figures). Cell division could not be detected, to any significant degree, during the course of the experiments. Experiments were performed using a Leica TCS SP2 AOBS (Leica, Wetzlar, Germany) confocal microscope with a × 10 objective. Cells were kept at 37 °C and 5% CO_2 for the all experiments, and a light image was taken every 2 h using the Leica software. Subsequent image analysis was performed using the ImageJ software (NIH, Bethesda, MD, USA) to quantify the percentage of wound reduction over time. To compare the percentage of cell migration, nonparametric unpaired *t*-test (Wilcoxon–Mann–Whitney) was used as a scoring method.

$[Ca^{2+}]_i$ measurements

BTEC and HMVEC-d were loaded with the acetoxymethyl ester form of fura-2 (2 μM fura-2 AM (Invitrogen), 45 min at 37 °C). Cells were seeded on gelatin-coated glass coverslips at a density of 5000 cells/cm^2 at 1–2 days before the experiments and starved in DMEM 5% FCS for at least 2 h before the experiments. Fluorescence measurements were made using a Polychrome V spectrofluorimeter (TILL Photonics, Munich BioRegio, Germany) attached to an Olympus × 51 microscope (Olympus, Tokyo, Japan) and Metafluor Imaging System (Molecular Devices, Sunnyvale, CA USA) (Liu *et al.*, 2006). During experiments, cells were maintained in standard extracellular solution of the following composition: 145mM NaCl, 5mM KCl, 2mM $CaCl_2$, 1mM $MgCl_2$, 10mM *N*-(2-hydroxyethyl)-piperazine-*N*′-ethanesufonic acid (HEPES), 10mM glucose (NaOH to pH 7.35). Cells were continuously bathed with a microperfusion system. Each fluorescence trace (340/380nm ratio) is representative of the traces seen in 50 cells obtained from at least two experiments. Student's *t*-test was used to statistically evaluate the data. The IgorPro software (Wavematrix, Lake Oswego, OR, USA) was used to further analyze the fluorescence trace to evaluate and use the agonist-induced slope change as a quantitative criterion to distinguish a cell response to an agonist from the background noise. One-way analysis of variance was performed to analyze data sets. *Post-hoc* tests were used to determine statistically significant differences among the groups (Student–Newman–Keuls test).

Immunofluorescence and confocal microscopy

For immunofluorescence, BTEC were transfected with TRPV4-GFP vector as described above. After 48 h, cells were fixed using 3% paraformaldehyde and permeabilized using cold methanol on dry ice. Staining of F-actin was achieved using the rhodamine-labeled phalloidin (Invitrogen). Images were collected using a Leica TCS SP2 AOBS confocal microscope and analyzed using ImageJ software. Control experiments were carried out

Author Manuscript Author Manuscript Author Manuscript Author Manuscript

without primary antibody. In each field, we chose the stress fiber focal plane and analyzed the field with a plot profile of the major cell axis. Quantifications of the plasma membrane localization of TRPV4 were carried out using the fluorescence signals within the first 5 μm from the top of the cell, and calculating the ratio between the 5 μm fluorescence value and the peak amplitude within the 5 μm. One-way analysis of variance was performed to analyze data sets. *Post-hoc* tests were used to determine statistically significant differences among the groups (Student–Newman–Keuls test). For the *in vivo* experiments (Supplementary Figure S3), BTEC were transfected with β-actin-mCherry vector. After 48 h, cells were perfused with standard extracellular solution (described above) in the presence of 10 μM 4αPDD. Cells were kept at 37 °C and 5% CO_2 for the all experiments, and confocal images were acquired before and at 10 and 15 min after 4αPDD perfusion using the Leica software.

Cell surface biotinylation

Cells were treated as required and incubated for 20 min with 1.5 mg/ml. Sulfo-NHS-LC-Biotin (Pierce) in 1 × phosphate-buffered saline (pH 8.0) on ice (Singh *et al.*, 2004). Following biotin-labeling, cells were washed and harvested in RIPA buffer (50mM Tris–HCl, 150mM NaCl, 0.1% sodium dodecyl sulfate, 0.5% sodium deoxycholate, 1% Triton X-100, 2mM EDTA, 1mM dithiothreitol, pH 7.4) supplemented with protease inhibitors as described earlier. Biotinylated proteins were pulled down with NeutrAvidin-linked beads (Pierce) and detected by western blotting. Band intensities of surface proteins were obtained using Quantity One 4.6.5 1D-analysis software (Bio-Rad, Hercules, CA, USA).

Online supplementary material

Supplementary Figure S1 shows the shTRPV4 and TRPV4-GFP constructs controls assessed in western blot and Ca^{2+}-imaging experiments. Lysates of HEK293 cells expressing TRPV4-GFP showed the expected ~90KDa band and a lower ~70 kDa band, which may correspond to endogenous TRPV4. As control, the anti-GFP antibody was also used to detect TRPV4-GFP, which shows up on the blot as the ~90 kDa band (Supplementary Figure S1C). In addition, lysate of BTEC cells transfected with shTRPV4 construct show the extent of TRPV4 knockdown, which was more than 50% after 72 h (Supplementary Figure S1D). Specificity of the anti-TRPV4 antibody was determined using the TRPV4 peptide and comparing its detection of TRPV4 with the two commercial TRPV4 antibodies (Chemicon and Alomone TRPV4 antibodies; Supplementary Figure S2). Experiments shown in Supplementary Figure S3 show that TRPV4 activation does not promote any actin remodeling by itself. BTEC were transfected with 1.5 μg of β-actin-mCherry vector (a kind gift from Dr Yamada) and live cell imaging was performed.

Supplementary Material

Refer to Web version on PubMed Central for supplementary material.

Acknowledgments

This work was supported by the University of Torino, Regione Piemonte (Ricerca Scientifica Applicata Sanita') and the National Institute of Dental and Craniofacial Research (Intramural Research). We thank Dr Kenneth Yamada (NIDCR, NIH, Bethesda, MD, USA) for the β-actin-mCherry and Dr Michael X. Zhu (Department of Physiology and Cell Biology, Ohio State University, OH, USA) for the TRPV4-GFP construct.

Author Manuscript Author Manuscript Author Manuscript Author Manuscript

References

Antoniotti S, Fiorio Pla A, Pregnolato S, Mottola A, Lovisolo D, Munaron L. Control of endothelial cell proliferation by calcium influx and arachidonic acid metabolism: a pharmacological approach. J Cell Physiol. 2003; 197:370–378. [PubMed: 14566966]

Becker D, Bereiter-Hahn J, Jendrach M. Functional interaction of the cation channel transient receptor potential vanilloid 4 (TRPV4) and actin in volume regulation. Eur J Cell Biol. 2009; 88:141–152. [PubMed: 19027987]

Becker D, Blase C, Bereiter-Hahn J, Jendrach M. TRPV4 exhibits a functional role in cell-volume regulation. J Cell Sci. 2005; 118:2435–2440. [PubMed: 15923656]

Bhati R, Patterson C, Livasy CA, Fan C, Ketelsen D, Hu Z, et al. Molecular characterization of human breast tumor vascular cells. Am J Pathol. 2008; 172:1381–1390. [PubMed: 18403594]

Birnbaumer L. The TRPC class of ion channels: a critical review of their roles in slow, sustained increases in intracellular Ca(2+) concentrations. Annu Rev Pharmacol Toxicol. 2009; 49:395–426. [PubMed: 19281310]

Boels K, Glassmeier G, Herrmann D, Riedel IB, Hampe W, Kojima I, et al. The neuropeptide head activator induces activation and translocation of the growth-factor-regulated Ca(2+)-permeable channel GRC. J Cell Sci. 2001; 114:3599–3606. [PubMed: 11707512]

Bussolati B, Deambrosis I, Russo S, Deregibus MC, Camussi G. Altered angiogenesis and survival in human tumor-derived endothelial cells. FASEB J. 2003; 17:1159–1161. [PubMed: 12709414]

Bussolati B, Grange C, Camussi G. Tumor exploits alternative strategies to achieve vascularization. Faseb J. 2011 (e-pub ahead of print).

Bussolati B, Grange C, Bruno S, Buttiglieri S, Deregibus MC, Tei L, et al. Neural-cell adhesion molecule (NCAM) expression by immature and tumor-derived endothelial cells favors cell organization into capillary-like structures. Exp Cell Res. 2006; 312:913–924. [PubMed: 16406048]

Carmeliet P. Angiogenesis in life, disease and medicine. Nature. 2005; 438:932–936. [PubMed: 16355210]

Collino F, Bussolati B, Gerbaudo E, Marozio L, Pelissetto S, Benedetto C, et al. Preeclamptic sera induce nephrin shedding from podocytes through endothelin-1 release by endothelial glomerular cells. Am J Physiol Renal Physiol. 2008; 294:F1185–F1194. [PubMed: 18287402]

Everaerts W, Nilius B, Owsianik G. The vanilloid transient receptor potential channel TRPV4: from structure to disease. Prog Biophys Mol Biol. 2010; 103:2–17. [PubMed: 19835908]

Fiorio Pla A, Grange C, Antoniotti S, Tomatis C, Merlino A, Bussolati B, et al. Arachidonic acid-induced Ca2+ entry is involved in early steps of tumor angiogenesis. Mol Cancer Res. 2008; 6:535–545. [PubMed: 18403634]

Fiorio Pla A, Genova T, Pupo E, Tomatis C, Genazzani A, Zaninetti R, et al. Multiple roles of protein kinase A on arachidonic acid-mediated Ca2+ entry and tumor-derived human endothelial cells migration. Mol Cancer Res. 2010; 8:1466–1476. [PubMed: 20870737]

Fiorio Pla A, Maric D, Brazer SC, Giacobini P, Liu X, Chang YH, et al. Canonical transient receptor potential 1 plays a role in basic fibroblast growth factor (bFGF)/FGF receptor-1-induced Ca2+ entry and embryonic rat neural stem cell proliferation. J Neurosci. 2005; 25:2687–2701. [PubMed: 15758179]

Fiorio Pla A, Munaron L. Calcium influx, arachidonic acid, and control of endothelial cell proliferation. Cell Calcium. 2001; 30:235–244. [PubMed: 11587547]

Folkman J. Fundamental concepts of the angiogenic process. Curr Mol Med. 2003; 3:643–651. [PubMed: 14601638]

Gao X, Wu L, O'Neil RG. Temperature-modulated diversity of TRPV4 channel gating: activation by physical stresses and phorbol ester derivatives through protein kinase C-dependent and-independent pathways. J Biol Chem. 2003; 278:27129–27137. [PubMed: 12738791]

Goswami C, Kuhn J, Heppenstall PA, Hucho T. Importance of non-selective cation channel TRPV4 interaction with cytoskeleton and their reciprocal regulations in cultured cells. PLoS ONE. 2010; 5:e11654. [PubMed: 20657843]

Author Manuscript Author Manuscript Author Manuscript Author Manuscript

Grange C, Bussolati B, Bruno S, Fonsato V, Sapino A, Camussi G. Isolation and characterization of human breast tumor-derived endothelial cells. Oncol Rep. 2006; 15:381–386. [PubMed: 16391858]

Hamdollah Zadeh MA, Glass CA, Magnussen A, Hancox JC, Bates DO. VEGF-mediated elevated intracellular calcium and angiogenesis in human microvascular endothelial cells *in vitro* are inhibited by dominant negative TRPC6. Microcirculation. 2008; 15:605–614. [PubMed: 18800249]

Hartmannsgruber V, Heyken WT, Kacik M, Kaistha A, Grgic I, Harteneck C, et al. Arterial response to shear stress critically depends on endothelial TRPV4 expression. PLoS ONE. 2007; 2:e827. [PubMed: 17786199]

Hida K, Hida Y, Amin DN, Flint AF, Panigrahy D, Morton CC, et al. Tumor-associated endothelial cells with cytogenetic abnormalities. Cancer Res. 2004; 64:8249–8255. [PubMed: 15548691]

Hyde CA, Missailidis S. Inhibition of arachidonic acid metabolism and its implication on cell proliferation and tumour-angiogenesis. Int Immunopharmacol. 2009; 9:701–715. [PubMed: 19239926]

Kwan HY, Huang Y, Yao X. TRP channels in endothelial function and dysfunction. Biochim Biophys Acta. 2007; 1772:907–914. [PubMed: 17434294]

Liedtke W, Kim C. Functionality of the TRPV subfamily of TRP ion channels: add mechano-TRP and osmo-TRP to the lexicon! Cell Mol Life Sci. 2005; 62:2985–3001. [PubMed: 16314934]

Liu X, Bandyopadhyay BC, Nakamoto T, Singh B, Liedtke W, Melvin JE, et al. A role for AQP5 in activation of TRPV4 by hypotonicity: concerted involvement of AQP5 and TRPV4 in regulation of cell volume recovery. J Biol Chem. 2006; 281:15485–15495. [PubMed: 16571723]

Ma X, Cao J, Luo J, Nilius B, Huang Y, Ambudkar IS, et al. Depletion of intracellular Ca2+ stores stimulates the translocation of vanilloid transient receptor potential 4-c1 heteromeric channels to the plasma membrane. Arterioscler Thromb Vasc Biol. 2010; 30:2249–2255. [PubMed: 20705915]

Meves H. Arachidonic acid and ion channels: an update. Br J Pharmacol. 2008; 155:4–16. [PubMed: 18552881]

Moes M, Boonstra J, Regan-Klapisz E. Novel role of cPLA(2)alpha in membrane and actin dynamics. Cell Mol Life Sci. 2010; 67:1547–1557. [PubMed: 20112044]

Morenilla-Palao C, Planells-Cases R, Garcia-Sanz N, Ferrer-Montiel A. Regulated exocytosis contributes to protein kinase C potentiation of vanilloid receptor activity. J Biol Chem. 2004; 279:25665–25672. [PubMed: 15066994]

Munaron L, Fiorio Pla A. Endothelial calcium machinery and angiogenesis: understanding physiology to interfere with pathology. Curr Med Chem. 2009; 16:4691–4703. [PubMed: 19903140]

Mutai H, Mann S, Heller S. Identification of chicken transmembrane channel-like (TMC) genes: expression analysis in the cochlea. Neuroscience. 2005; 132:1115–1122. [PubMed: 15857715]

Nie D, Honn KV. Cyclooxygenase, lipoxygenase and tumor angiogenesis. Cell Mol Life Sci. 2002; 59:799–807. [PubMed: 12088280]

Nilius B, Owsianik G, Voets T, Peters JA. Transient receptor potential cation channels in disease. Physiol Rev. 2007; 87:165–217. [PubMed: 17237345]

Patton AM, Kassis J, Doong H, Kohn EC. Calcium as a molecular target in angiogenesis. Curr Pharm Des. 2003; 9:543–551. [PubMed: 12570802]

Peppelenbosch MP, Qiu RG, de Vries-Smits AM, Tertoolen LG, de Laat SW, McCormick F, et al. Rac mediates growth factor-induced arachidonic acid release. Cell. 1995a; 81:849–856. [PubMed: 7781062]

Peppelenbosch MP, Tertoolen LG, Van der Flier A, De Laat SW. Evaluation of single-channel gating kinetics produced after amplitude-based separation of unitary currents. J Neurosci Methods. 1995b; 58:49–59. [PubMed: 7475233]

Pocock TM, Foster RR, Bates DO. Evidence of a role for TRPC channels in VEGF-mediated increased vascular permeability *in vivo*. Am J Physiol Heart Circ Physiol. 2004; 286:H1015–H1026. [PubMed: 14551041]

Prevarskaya N, Skryma R, Shuba Y. Ion channels and the hallmarks of cancer. Trends Mol Med. 2010; 16:107–121. [PubMed: 20167536]

Author Manuscript Author Manuscript Author Manuscript Author Manuscript

Roberts LA, Glenn H, Hahn CS, Jacobson BS. Cdc42 and RhoA are differentially regulated during arachidonate-mediated HeLa cell adhesion. J Cell Physiol. 2003; 196:196–205. [PubMed: 12767056]

Shin EA, Kim KH, Han SI, Ha KS, Kim JH, Kang KI, et al. Arachidonic acid induces the activation of the stress-activated protein kinase, membrane ruffling and H2O2 production via a small GTPase Rac1. FEBS Lett. 1999; 452:355–359. [PubMed: 10386621]

Singh BB, Lockwich TP, Bandyopadhyay BC, Liu X, Bollimuntha S, Brazer SC, et al. VAMP2-dependent exocytosis regulates plasma membrane insertion of TRPC3 channels and contributes to agonist-stimulated Ca2+ influx. Mol Cell. 2004; 15:635–646. [PubMed: 15327778]

St Croix B, Rago C, Velculescu V, Traverso G, Romans KE, Montgomery E, et al. Genes expressed in human tumor endothelium. Science. 2000; 289:1197–1202. [PubMed: 10947988]

Suzuki M, Hirao A, Mizuno A. Microtubule-associated [corrected] protein 7 increases the membrane expression of transient receptor potential vanilloid 4 (TRPV4). J Biol Chem. 2003; 278:51448–51453. [PubMed: 14517216]

Thodeti CK, Matthews B, Ravi A, Mammoto A, Ghosh K, Bracha AL, et al. TRPV4 channels mediate cyclic strain-induced endothelial cell reorientation through integrin-to-integrin signaling. Circ Res. 2009; 104:1123–1130. [PubMed: 19359599]

Troidl C, Troidl K, Schierling W, Cai WJ, Nef H, Mollmann H, et al. Trpv4 induces collateral vessel growth during regeneration of the arterial circulation. J Cell Mol Med. 2009; 13:2613–2621. [PubMed: 19017361]

Tsai MH, Hall A, Stacey DW. Inhibition by phospholipids of the interaction between R-ras, rho, and their GTPase-activating proteins. Mol Cell Biol. 1989; 9:5260–5264. [PubMed: 2513485]

Van Buren JJ, Bhat S, Rotello R, Pauza ME, Premkumar LS. Sensitization and translocation of TRPV1 by insulin and IGF-I. Mol Pain. 2005; 1:17. [PubMed: 15857517]

Waning J, Vriens J, Owsianik G, Stuwe L, Mally S, Fabian A, et al. A novel function of capsaicin-sensitive TRPV1 channels: involvement in cell migration. Cell Calcium. 2007; 42:17–25. [PubMed: 17184838]

Watanabe H, Davis JB, Smart D, Jerman JC, Smith GD, Hayes P, et al. Activation of TRPV4 channels (hVRL-2/mTRP12) by phorbol derivatives. J Biol Chem. 2002; 277:13569–13577. [PubMed: 11827975]

Watanabe H, Vriens J, Prenen J, Droogmans G, Voets T, Nilius B. Anandamide and arachidonic acid use epoxyeicosatrienoic acids to activate TRPV4 channels. Nature. 2003; 424:434–438. [PubMed: 12879072]

Yu PC, Gu SY, Bu JW, Du JL. TRPC1 is essential for *in vivo* angiogenesis in zebrafish. Circ Res. 2010; 106:1221–1232. [PubMed: 20185799]

Author Manuscript
Author Manuscript
Author Manuscript
Author Manuscript

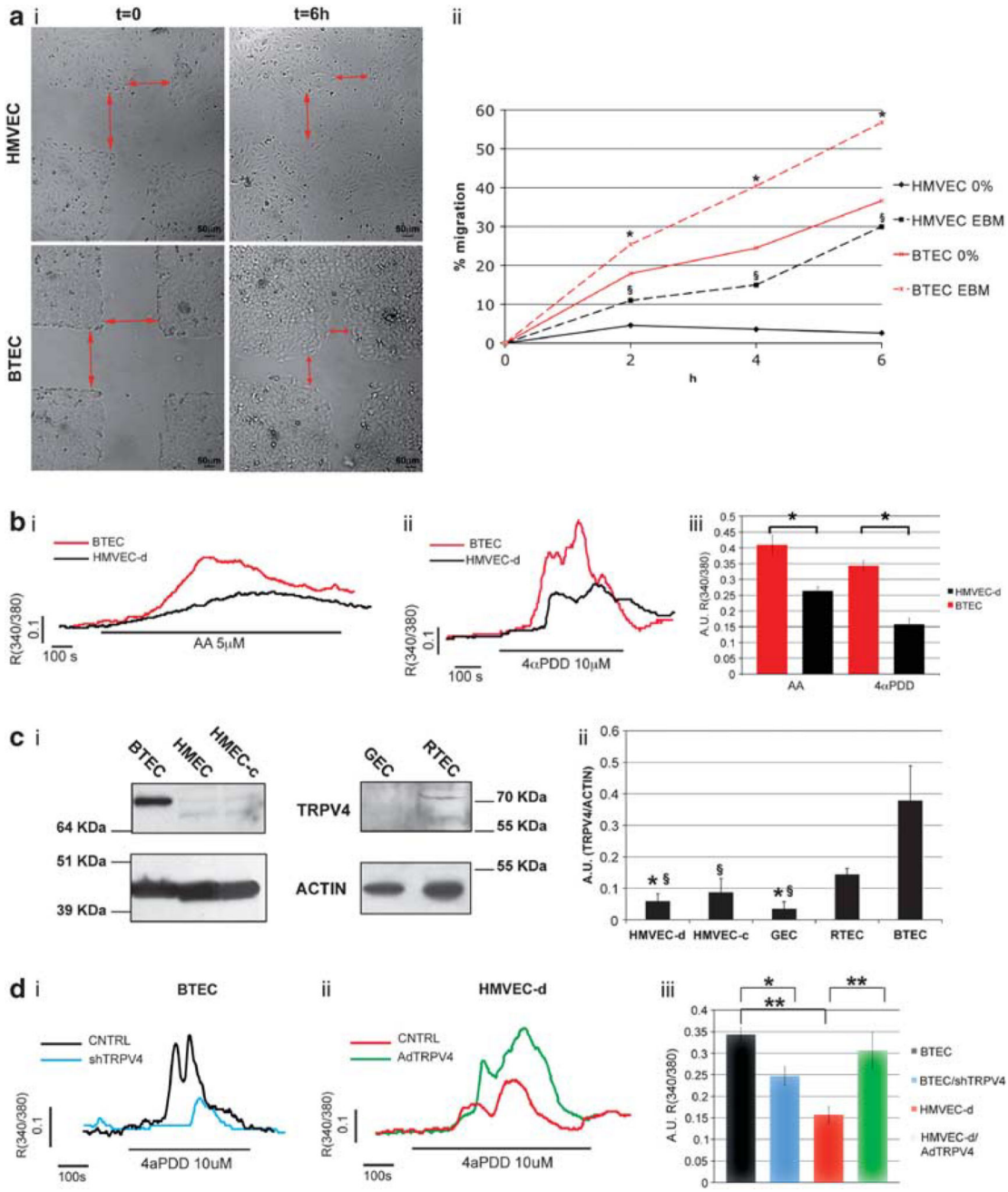

Figure 1.

TRPV4 is differentially expressed and functional in normal and tumor-derived endothelial cells. (**a**) (i) Representative pictures showing the wound healing at the beginning ($t = 0$ h) and 6 h after the wound in normal endothelial cells (HMVEC-d) and breast tumor derived ECs (BTEC). (ii) Percentage of migration of BTEC and HMVEC-d in high (EBM) and serum-free (0%) within 6 h. The symbols * and § represent significant difference relative to 0% BTEC and 0% HMVEC-d, respectively. $P < 0.05$ (Wilcoxon test). (**b**) AA (i) and 4αPDD-induced (ii) Ca^{2+} responses in BTEC (red trace) and HMVEC-d (black trace). (iii) Bar graph summarizing the relative quantification of the peak amplitude of AA- or 4αPDD-

Author Manuscript Author Manuscript Author Manuscript Author Manuscript

induced $[Ca^{2+}]_i$ responses. The symbol * represent significant difference $P<0.01$, (Student's *t*-test). (**c**) (i) TRPV4 and actin expression in normal human microvascular ECs (HMEVC-d, HMEVC-c and GEC) and tumor-derived ECs (RTEC, BTEC). (ii) Relative TRPV4 expression, normalized to actin expression. The symbols * and § represent significant difference relative to RTEC and BTEC respectively $P<0.05$ (Student's *t*-test). (**d**) 4αPDD-induced Ca^{2+} i responses in control (CNTRL) and shTRPV4-transfected BTEC (i) and in control (CNTRL) and TRPV4 overexpressing (AdTRPV4) HMVEC-d (ii). (iii) Bar graph summarizing the relative quantification of the peak amplitude of 4αPDD-induced Ca^{2+} i responses. The symbols * and ** represents significant difference $P<0.05$ and 0.01, respectively, (Student's *t*-test).

Author Manuscript Author Manuscript Author Manuscript Author Manuscript

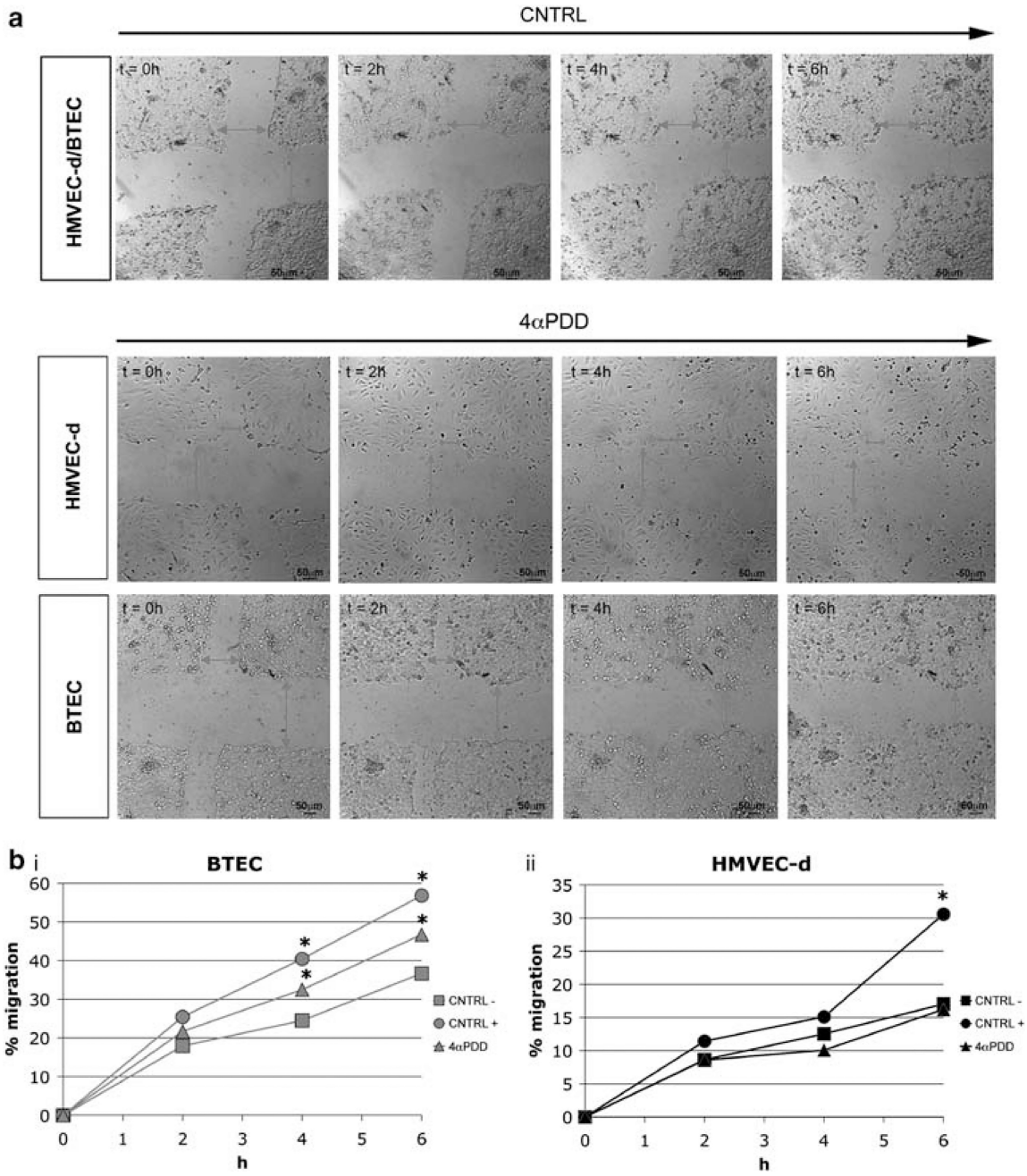

Figure 2.

TRPV4 activation promotes tumor-derived but not normal EC migration. Wound healing assays performed both on BTEC and HMVEC-d. (**a**) Representative picture showing the wound healing in control (CNTRL) and 4αPDD-treated cells at the beginning ($t = 0$ h), and at 2, 4 and 6 h after wounding in HMVEC-d and BTEC. (**b**) Percentage of migrating BTEC (i) and HMVEC-d (ii) in EBM 0% FCS (CNTRL−; **b**i) and EBM 2% FCS (CNTRL−; **b**ii), 10 μM 4αPDD-treated cells (4αPDD) and EBM 10% FCS as positive control (CNTRL+). The symbol * represents significant difference relative to CNTRL. $P < 0.05$ (Wilcoxon test).

Data are expressed as the mean ± s.e.m. A full colour version of this figure is available at the *Oncogene* journal online.

Author Manuscript Author Manuscript Author Manuscript Author Manuscript

Author Manuscript Author Manuscript Author Manuscript Author Manuscript

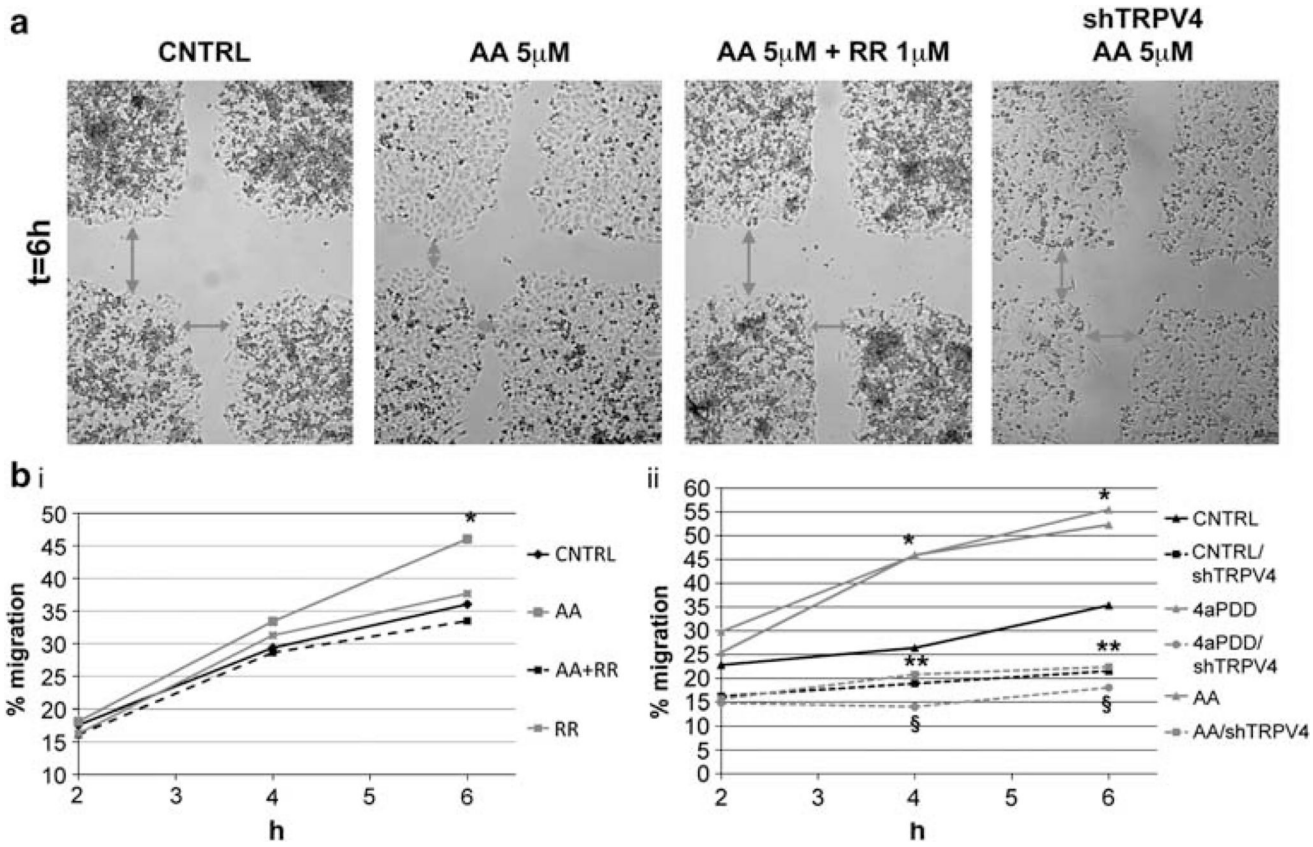

Figure 3.

AA-induced B-TEC migration is mediated by TRPV4 activation. Wound-healing experiments on BTEC. (**a**) Representative pictures showing BTEC wound healing after 6 h treatment in control (CNTRL), and shTRPV4-transfected BTEC in the presence or absence of 5 μM AA and 1 μM ruthenium red (RR). (**b**) Percentage of BTEC migration starting from 2 h after wounding. (i) RR (1 μM) completely reverses AA-induced BTEC migration 6 h after wounding. CNTRL: BTEC in the presence of DMEM 0%FCS; AA: BTEC stimulated with 5 μM AA; AA+RR: BTEC in DMEM 0% FCS stimulated with 5 μM AA in the presence of 1 μM RR; RR: BTEC in DMEM 0% FCS in the presence of 1 μM RR. (ii) 5 μM AA and 10 μM 4αPDD were not able to exert any migratory effect in shTRPV4-transfected BTEC. CNTRL: BTEC transfected with empty shRNA vector in DMEM 0% FCS; shTRPV4: BTEC transfected with shTRPV4 vector in DMEM 0% FCS; 4αPDD: BTEC transfected with empty shRNA vector in DMEM 0% FCS and stimulated with 10 μM 4αPDD; 4αPDD/ shTRPV4: BTEC transfected with shTRPV4 vector in DMEM 0% FCS and stimulated with 10 μM 4αPDD; AA: BTEC transfected without vector in DMEM 0% FCS and stimulated with 5 μM AA; AA/shTRPV4: BTEC transfected with shTRPV4 vector in DMEM 0% FCS and stimulated with 5 μM AA; *, ** and § represent significant differences relative to CNTRL, AA and 4αPDD, respectively. $P < 0.05$ (Wilcoxon test). Data are expressed as the mean value. A full colour version of this figure is available at the *Oncogene* journal online.

Author Manuscript Author Manuscript Author Manuscript Author Manuscript

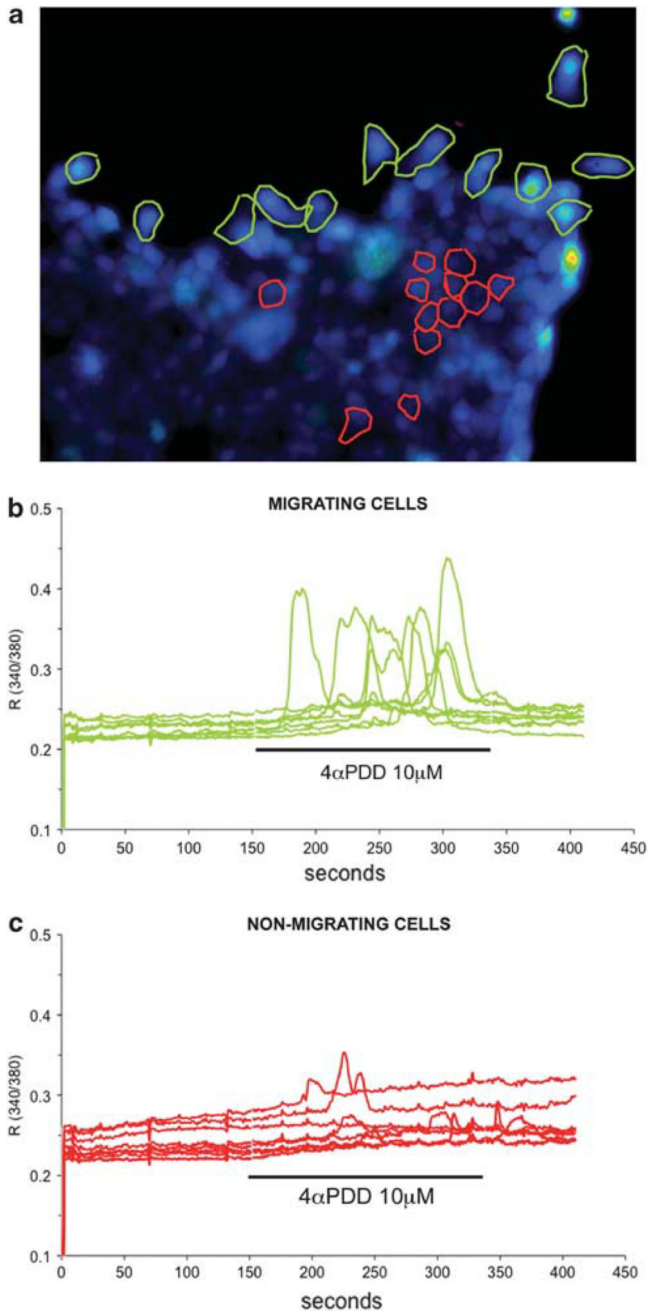

Figure 4.

TRPV4-mediated Ca^{2+} responses in migrating versus non-migrating cells. 4αPDD-induced Ca^{2+} responses in BTEC grown to confluence and wounded in serum-free medium. Ca^{2+}-imaging experiments were performed 2 h after wounding. (**a**) Representative image in pseudocolor showing regions of interest (ROIs) representing cells on the wound edges (green ROIs) or 'inside' the wound (red ROIs). (**b, c**) 4αPDD-induced Ca^{2+} responses in migrating cells on the wound edge (**b**) or non-migrating cells inside the wound (**c**). Each trace represents the ratio (340/380 nm) of a single cell in the field.

Author Manuscript Author Manuscript Author Manuscript Author Manuscript

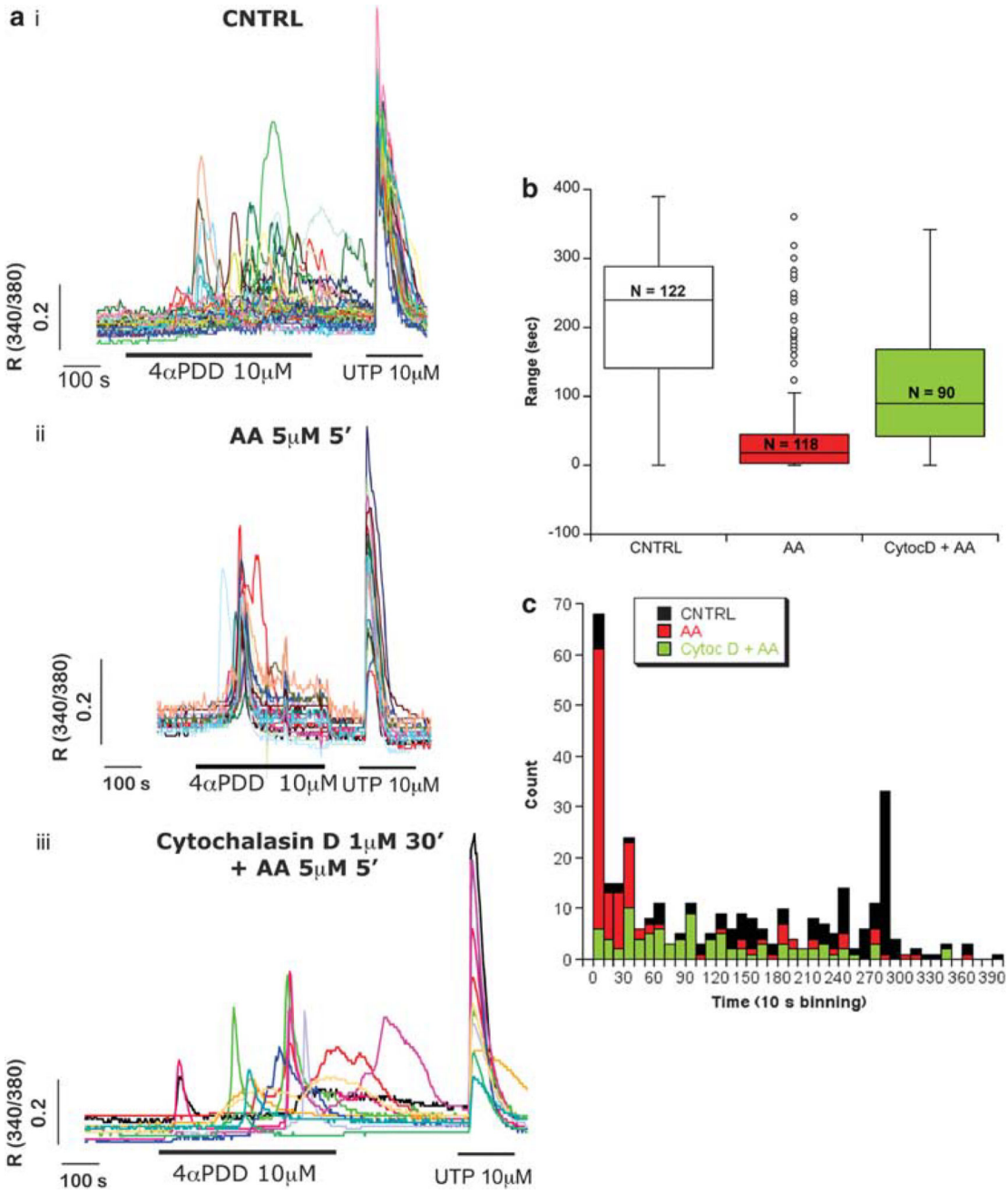

Figure 5.

AA synchronizes TRPV4-mediated Ca^{2+} responses. (**a**) 4αPDD-induced Ca^{2+} responses in BTEC population in control (CNTRL). (i) BTEC pre-incubated in the presence of 5 μM AA with (iii) or without (ii) 1 μM cytochalasin D. Each trace represents the ratio (340/380 nm) of a single cell in the field. At the end of the experiment, BTEC were perfused with 10 μM uridine triphosphate as positive control. (**b**) Boxplot of the latency of 4αPDD-induced Ca^{2+} responses (relative to the first response) in control (same conditions as **a**i), BTEC preincubated in the presence of 5 μM AA with (same as **a**iii, CytoD+AA) or without (same as **a**ii, AA) 1 μM cytochalasin D. Numbers in the boxes are the number of cells used in

Author Manuscript Author Manuscript Author Manuscript Author Manuscript

calculating for each condition. (**c**) Distribution of the latency of 4αPDD-induced Ca^{2+} responses relative to the first response in the same conditions as in **a** and **b**. The time latency was binned at 10 s. TRPV4-mediated tumor derived endothelial cell migration

Author Manuscript Author Manuscript Author Manuscript Author Manuscript

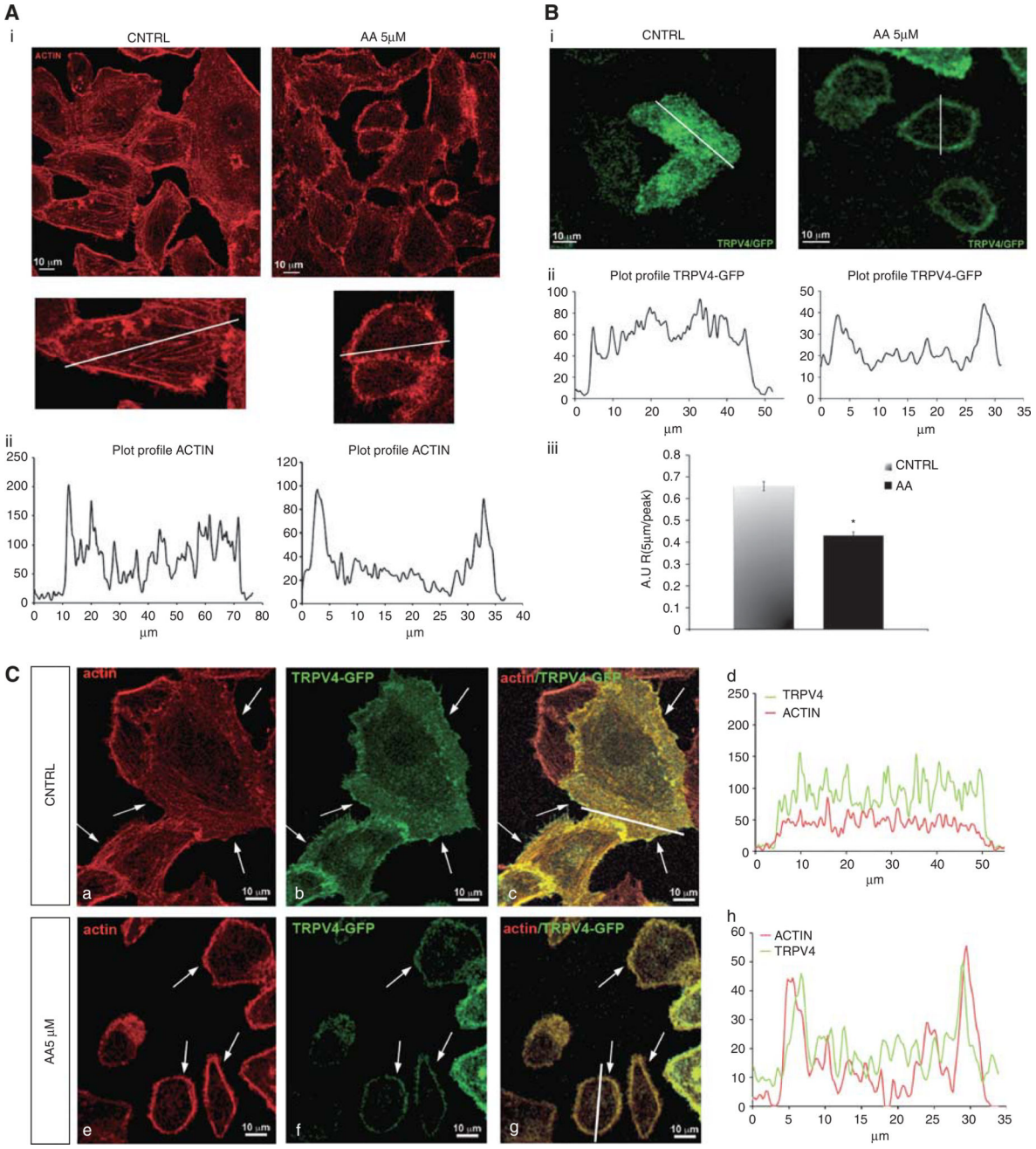

Figure 6.

AA induces actin remodeling with consequent increase of TRPV4 expression at the cell surface. (**A**) (i) Representative images showing actin expression in control (CNTRL) and after 5 μM AA perfusion (AA). (ii) Plot profile of the phalloidin-Texas Red fluorescence intensity along the major axis (white lines) of the cells. BTEC were fixed in control and after incubation with 5 μM AA (10 min, 37 °C), and stained for phalloidin-Texas Red to detect actin. (**B**) (i) Representative images showing TRPV4 localization in control (CNTRL) and after incubation with 5 μM AA (AA). (ii) Plot profile of the TRPV4-GFP fluorescence intensity along the axis of the cell (white lines). (iii) Quantification of the TRPV4-GFP

Author Manuscript Author Manuscript Author Manuscript Author Manuscript

fluorescence intensity at 5 μm from the beginning of the cell relative to the peak amplitude within the 5 μm depth. (n = 163 cells for control condition and n = 197 cells for AA condition). The symbol * represents significant difference relative to control, P <0.0001 (Wilcoxon test). Data are expressed as the mean ± s.e.m. (**C**) Localization of TRPV4-GFP (green; panels b and f) and phalloidin-Texas Red to stain actin (red; panels a and e) in the presence (panels e–h) or absence (panels a–c) of 5 μM AA. Panels c and g represent overlay images between actin (red) and TRPV4 (green). Graphs d and h show the fluorescence intensity profiles, which indicate the extent of TRPV4 and actin colocalization as determined along the area marked by the white lines.

Author Manuscript Author Manuscript Author Manuscript Author Manuscript

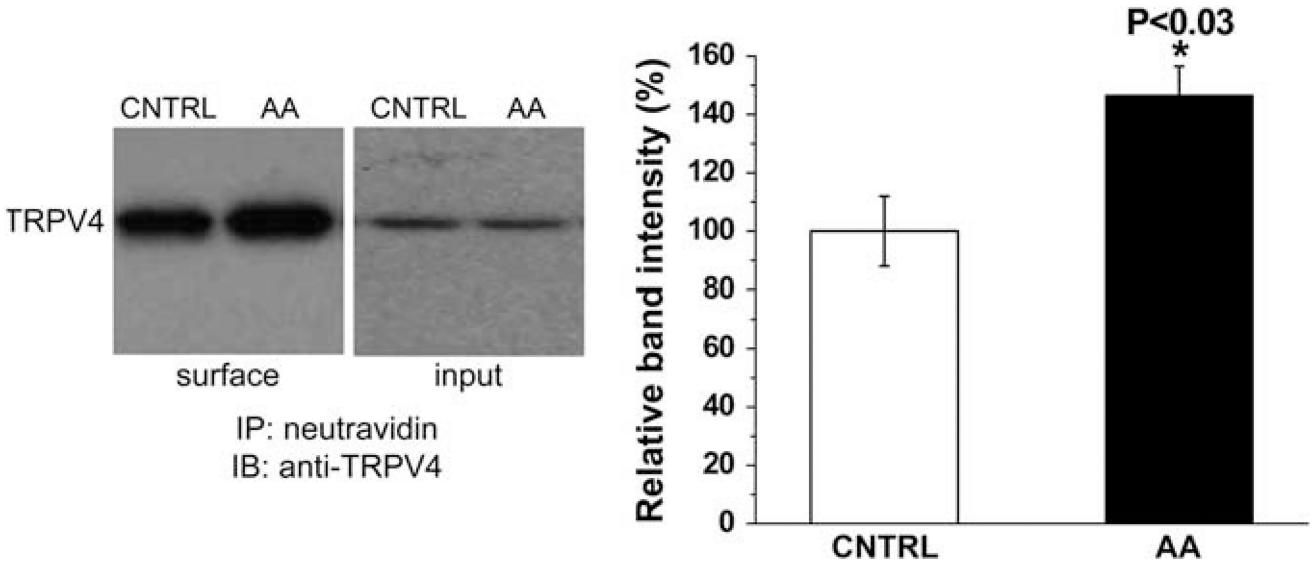

Figure 7.

Increased surface expression of TRPV4 following treatment with arachidonic acid. Cells were serum-starved for 2 h and then treated with AA for 10 min at 37 °C. As control, cells were only serum-starved. Following stimulation, cells were biotinylated and then harvested. Lysates were immunoprecipitated using neutravidin beads and TRPV4 was detected in western blot using the anti-TRPV4 antibody. The right panel of the blot shows the input levels, whereas the left panel shows TRPV4 detection in untreated control (CNTRL) and AA-treated (AA) cells. Band intensities were quantified and the histogram shows the average intensity values (mean ± s.e.m.) for TRPV4 bands detected in control and AA-treated cells in 4 different immunoprecipitation experiments. The intensity value for control cells was set to 100% and the value for AA-treated cells was expressed relative to control cells. Statistical analysis was conducted using the Student's *t*-test and showed a significant increase in TRPV4 band intensity with AA treatment (*, $P < 0.03$).